Journal of Non-Newtonian Fluid Mechanics 319 (2023) 105074

Contents lists available at ScienceDirect

Journal of Non-Newtonian Fluid Mechanics

journal homepage: www.elsevier.com/locate/jnnfm

The analytical solution for the flow of a Papanastasiou fluid in ducts with variable geometry

Kostas D. Housiadas [a,*], Georgios C. Georgiou [b]

[a] Department of Mathematics, University of the Aegean, Karlovassi 83200, Samos, Greece
[b] Department of Mathematics and Statistics, University of Cyprus, P.O. Box 20537, 1678 Nicosia, Cyprus

ARTICLE INFO

Keywords:
Bingham fluid
Papanastasiou fluid
Lubrication approximation
Undulating channels and pipes
Lambert w function
Pressure drop

ABSTRACT

We solve the isothermal, steady and creeping flow of the regularized Papanastasiou model in ducts, such as symmetric channels and axisymmetric pipes, with varying rigid walls. The classic lubrication approximation is invoked to simplify the governing equations and to produce an exact analytical solution for the flow field with the aid of the Lambert *W* function. For specific suitable values of the parameters of the Papanastasiou model, the solution reduces to the corresponding exact analytical solutions for the ideal yield-stress Bingham and Newtonian fluids. The analytical solutions derived here are used to calculate the average pressure drop required to maintain the constant volumetric flowrate through the duct. Results are provided for symmetric undulating or linearly varying channels with the emphasis put on the effects of the Bingham and regularization numbers, and the amplitude of the undulation or the wall variation, respectively.

1. Introduction

Yield-stress (or viscoplastic) materials include various classes of materials, such as colloidal gels, emulsions, soft glassy materials, and jammed noncolloidal suspensions, foams, and paints [1,2]. They have received considerable attention in the past few decades as they appear in many industrial processes, such as food processing, pharmaceutics, cosmetics, and oil-drilling and transport [3]. They also appear in construction, in geophysical flows and in biological flows [4]. Ideal yield-stress fluids behave as solids below the so-called "yield stress", τ_0^*, and as fluids otherwise. The most popular constitutive equation describing viscoplastic behavior is the ideal Bingham model [5]:

$$\begin{cases} \dot{\gamma}^* = \mathbf{0}, & \tau^* \le \tau_0^* \\ \tau^* = \left(\mu_0^* + \tau_0^*/\dot{\gamma}^*\right)\dot{\gamma}^*, & \tau^* > \tau_0^* \end{cases} \tag{1}$$

where μ_0^* is the viscoplastic viscosity, $\dot{\gamma}^*$ is the symmetric rate-of-deformation tensor, $\dot{\gamma}^* = \nabla^*\mathbf{v}^* + (\nabla^*\mathbf{v}^*)^T$, and $\dot{\gamma}^* > 0$ is the second invariant of $\dot{\gamma}^*$; note that throughout this paper symbols with stars denote dimensional quantities. Generally, the second invariant of a symmetric second-order tensor, $\mathbf{X}$, (also referred to as "the magnitude of the tensor") is defined as $X \equiv \| \mathbf{X} \| := \sqrt{\mathbf{X} : \mathbf{X}/2} > 0$ unless $X = 0 \Leftrightarrow \mathbf{X} = \mathbf{0}$. Based on this definition, $\tau^* = \sqrt{\tau^* : \tau^*/2}$ and $\dot{\gamma}^* = \sqrt{\dot{\gamma}^* : \dot{\gamma}^*/2}$; thus, in simple shear flow $\dot{\gamma}^*$ coincides with the externally imposed shear-rate.

Solving ideal viscoplastic flows requires the determination of the unyielded ($\tau^* \le \tau_0^*$) and yielded ($\tau^* > \tau_0^*$) zones, $\Omega_{unyielded}$ and $\Omega_{yielded}$, respectively, where the two branches of the constitutive model, as shown in Eq. (1), apply. This can easily be determined only in simple unidirectional flows, while in two- and three-dimensional flows this may be a formidable task [2,6]. Due to this difficulty, various modifications (or regularizations) of the ideal Bingham model have been proposed and used in the literature. The purpose is the replacement of the unyielded region with another which deforms much slower than the yielded region [6]. Thus, the material deforms everywhere in the flow domain and the calculation of the unyielded region is not required. One of the popular regularized models is the Papanastasiou model [7], given by:

$$\begin{aligned} \tau^* &= \eta^*(\dot{\gamma}^*)\,\dot{\gamma}^* \\ \eta^*(\dot{\gamma}^*) &= \mu_0^* + \frac{\tau_0^*}{\dot{\gamma}^*}\left(1 - \exp(-m^*\dot{\gamma}^*)\right) \end{aligned} \tag{2}$$

where $\eta^* = \eta^*(\dot{\gamma}^*)$ is the apparent viscosity and $m^* \ge 0$ is a parameter. Eq. (2) is a non-linear generalized Newtonian model whose viscosity depends on the magnitude of $\dot{\gamma}^*$. For sufficiently large values of m^* Eq.

* Corresponding author.
E-mail address: housiada@aegean.gr (K.D. Housiadas).

https://doi.org/10.1016/j.jnnfm.2023.105074
Received 19 March 2023; Received in revised form 28 April 2023; Accepted 25 May 2023
Available online 29 May 2023

(2) reduces to Eq. (1). When m^* goes to zero, or when τ_0^* goes to zero, both the ideal Bingham and Papanastasiou models reduce to the simple Newtonian model:

$$\tau^* = \mu_0^* \dot{\gamma}^* \tag{3}$$

The objective of the present work is to solve analytically the laminar flow of a Papanastasiou fluid in a symmetric duct (such as a symmetric channel with respect to the midplane, and an axisymmetric pipe). For both geometries, the cross-section varies with the distance from the inlet plane, while the shape of the wall(s) is fixed, and a-priori described in general with a known and smooth (continuous and differentiable) function. Due to the varying cross-section, the flow fields for both geometric configurations are two-dimensional (2D) and bidirectional. We use the Papanastasiou model to avoid determining a yield surface and a plug zone. We do not solve the full governing equations since this would require a numerical method to handle the strongly non-linear terms; the latter appear in the mathematical model because the apparent viscosity depends on all the components of the rate of deformation tensor (see Eq. (2)). Instead, we invoke the classic lubrication approximation, valid for long ducts, to simplify the equations. The final equations are solved analytically for the two velocity components and the pressure gradient by means of the Lambert W function (see subsection 3.3. for more details).

A well-known limitation of the standard lubrication method when applied to viscoplastic flows is the lubrication paradox [6,8,9]. It turns out that at leading order, a plug velocity that varies slowly in the flow direction is predicted and the shape of the yield surface is incorrect. For example, in a converging channel the unyielded core appears to also be converging, which violates the conservation of mass. The lubrication paradox can be avoided by resorting to the lubrication approach of Fusi and co-workers [10–12], or it can be overcome by proceeding to high-order asymptotic solutions, as suggested by Frigaard and Ryan [8] and Putz et al. [9]. Both methods are extensively reviewed in Ref. [12].

The rest of the paper is organized as follows. The governing equations and boundary and other auxiliary conditions are described in Section 2 for both symmetric channels and pipes. The dimensionless equations are simplified by means of the lubrication approximation in Section 3, albeit the final equations are still two-dimensional. The analytical solutions for the 2D flow-field (velocity components and pressure gradient) at the leading-order of approximation are then derived. For completeness the analytical solutions for the Newtonian and ideal Bingham fluids are also presented. In Section 4, the general expression for the pressure drop is derived in terms of the wall(s) shape function for both channels and pipes. In section 5, we present and discuss results for undulating and linearly varying ducts. Finally, the concluding remarks are given in Section 6.

2. Problem definition

We consider the isothermal, steady-state creeping flow of an incompressible Bingham-Papanastasiou fluid in a duct (channel or tube) with length L^* and variable cross-section. The height of the symmetric channel and the radius of the cross-section of the axisymmetric pipe are allowed to vary with the distance from the inlet plane. Both are described with the aid of the shape function $h^* = h^*(z^*)$ which is known and fixed in advance; note that $h_0^* \equiv h^*(0)$ and $h_f^* \equiv h^*(L^*)$. Cartesian and cylindrical coordinates are employed for the channel and pipe flows as illustrated in Fig. 1. Gravity and other external forces are neglected, and the flow is assumed to be driven solely by the constant volumetric flow-rate at the inlet plane, Q^*. With these assumptions the velocity vector for both flows is of the form $\mathbf{v}^* = v^*(y^*, z^*)\mathbf{e}_y + u^*(y^*, z^*)\mathbf{e}_z$. For both geometries we will be referring to u^* as the "axial velocity component" and to v^* as the "transverse velocity component".

For the channel flow, the volumetric flow-rate per unit length in the neutral direction is given as

$$Q^* = \int_{-h^*(z^*)}^{h^*(z^*)} u^*(y^*, z^*)dy^* = 2\int_0^{h^*(z^*)} u^*(y^*, z^*)dy^*$$

where in the second equality, the symmetry with respect to the midplane has been taken into account. For the pipe flow, the volumetric flow-rate is $Q^* = 2\pi \int_0^{h^*(z^*)} y^* u^*(y^*, z^*)dy^*$.

It is preferable to work with dimensionless equations. To this end, z^* is scaled by L^*, y^* and h^* by h_0^*, u^* by U^*, v^* by $U^* h_0^*/L^*$, p^* by $\mu_0^* U^* L^*/h_0^{*2}$, and the extra-stress components by $\mu_0^* U^*/h_0^*$, where U^* is the mean axial velocity, defined by

$$U^* = \begin{cases} \dfrac{Q^*}{2h_0^*}, \text{channel} \\ \dfrac{Q^*}{2\pi h_0^{*2}}, \text{tube} \end{cases} \tag{4}$$

Three dimensionless numbers arise when the above characteristic scales are used: the aspect ratio of the duct, ε, the Bingham number, Bn, and the regularization parameter, M, defined as follows:

$$\varepsilon \equiv \frac{h_0^*}{L^*}, \quad Bn \equiv \frac{\tau_0^* h_0^*}{\mu_0^* U^*}, \quad M \equiv \frac{m^* U^*}{h_0^*} \tag{5}$$

The dimensionless flow domain for both channels and pipes is:

$$\Omega = \{(y, z) | 0 < z < 1, \ 0 < y < h(z)\}$$

where for the channel flow, we consider only the upper half of the domain due to the symmetry with respect to the midplane. The standard no-slip, no-penetration condition is applied at the wall, while symmetry conditions are employed at the midplane or the axis of symmetry:

$$v = u = 0 \quad \text{at} \quad y = h(z), \ 0 \le z \le 1 \tag{6}$$

$$v = \frac{\partial u}{\partial y} = 0 \quad \text{at} \quad y = 0, \ 0 \le z \le 1 \tag{7}$$

Given that the flow is assumed to be incompressible, the volumetric flow

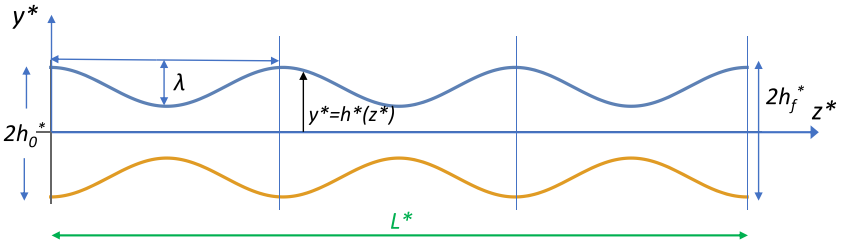

Fig. 1. Geometry and Cartesian coordinate system (y^*,z^*) for a symmetric undulating channel with three undulations ($k = 3$), of aspect ratio $\varepsilon = h_0^*/L^* = 0.2$ and amplitude $\lambda = 0.4$.

rate is independent of the axial distance z and thus:

$$\int_0^{h(z)} y^q\, u(y,z)\, dy = 1, \quad 0 \le z \le 1 \tag{8}$$

In Eq. (8) and hereafter, the geometric parameter q is used for succinctness, where $q = 0$ for the channel and $q = 1$ for the pipe.

2.1. Channel flow

The continuity equation and the two components of the momentum equation become:

$$\frac{\partial u}{\partial z} + \frac{\partial v}{\partial y} = 0 \tag{9}$$

$$-\frac{\partial p}{\partial z} + \varepsilon \frac{\partial \tau_{zz}}{\partial z} + \frac{\partial \tau_{yz}}{\partial y} = 0 \tag{10}$$

$$-\frac{\partial p}{\partial y} + \varepsilon^2 \frac{\partial \tau_{yz}}{\partial z} + \varepsilon \frac{\partial \tau_{yy}}{\partial y} = 0 \tag{11}$$

$$\begin{aligned} \tau_{yz} &= \eta \left(\frac{\partial u}{\partial y} + \varepsilon^2 \frac{\partial v}{\partial z} \right) \\ \tau_{yy} &= 2\varepsilon\, \eta \frac{\partial v}{\partial y} \\ \tau_{zz} &= 2\varepsilon\, \eta \frac{\partial u}{\partial z} \end{aligned} \tag{12}$$

where the apparent viscosity $\eta = \eta(\dot\gamma)$ is given as:

$$\eta(\dot\gamma) = 1 + \frac{Bn}{\dot\gamma}(1 - \exp(-M\dot\gamma)) \tag{13}$$

and

$$\dot\gamma = \sqrt{4\varepsilon^2 \left(\frac{\partial u}{\partial z} \right)^2 + \left(\varepsilon^2 \frac{\partial v}{\partial z} + \frac{\partial u}{\partial y} \right)^2} \tag{14}$$

In the above equation, $\partial v/\partial y$ has been eliminated by means of Eq. (9).

2.2. Pipe flow

The governing equations for pipe flow read as follows:

$$\frac{\partial u}{\partial z} + \frac{\partial v}{\partial y} + \frac{v}{y} = 0 \tag{15}$$

$$-\frac{\partial p}{\partial z} + \varepsilon \frac{\partial \tau_{zz}}{\partial z} + \frac{\partial \tau_{yz}}{\partial y} + \frac{\tau_{yz}}{y} = 0 \tag{16}$$

$$-\frac{\partial p}{\partial y} + \varepsilon^2 \frac{\partial \tau_{yz}}{\partial z} + \varepsilon \left(\frac{\partial \tau_{yy}}{\partial y} + \frac{\tau_{yy} - \tau_{\theta\theta}}{y} \right) = 0 \tag{17}$$

$$\begin{aligned} \tau_{yz} &= \eta \left(\frac{\partial u}{\partial y} + \varepsilon^2 \frac{\partial v}{\partial z} \right) \\ \tau_{yy} &= 2\varepsilon\, \eta \frac{\partial v}{\partial y} \\ \tau_{zz} &= 2\varepsilon\, \eta \frac{\partial u}{\partial z} \\ \tau_{\theta\theta} &= 2\varepsilon\, \eta \frac{v}{y} \end{aligned} \tag{18}$$

where the apparent viscosity $\eta = \eta(\dot\gamma)$ is given as:

$$\eta(\dot\gamma) = 1 + \frac{Bn}{\dot\gamma}(1 - \exp(-M\dot\gamma)) \tag{19}$$

and

$$\dot\gamma = \sqrt{2\varepsilon^2 \left(\left(\frac{\partial u}{\partial z} \right)^2 + \left(\frac{\partial v}{\partial y} \right)^2 + \left(\frac{v}{y} \right)^2 \right) + \left(\varepsilon^2 \frac{\partial v}{\partial z} + \frac{\partial u}{\partial y} \right)^2} \tag{20}$$

3. Lubrication approximation and solutions

For long ducts, the aspect ratio is a small parameter, $0 < \varepsilon << 1$, and thus the governing equations and accompanying auxiliary conditions (boundary, symmetry and integral conditions) can be simplified considerably. Indeed, in the limit of a vanishing aspect ratio ($\varepsilon \to 0$), Eq. (11) for the channel flow and Eq. (17) for the pipe flow show that $p = p(z)$ only. Also, the components of the constitutive model give $\tau_{yy} = \tau_{zz} = 0$, $\tau_{\theta\theta} = 0$ (for the pipe only), and $\dot\gamma = |\partial u/\partial y| > 0$. Hence, the non-trivial governing equations are:

$$\frac{\partial u}{\partial z} + \frac{1}{y^q} \frac{\partial}{\partial y}(y^q v) = 0 \tag{21}$$

$$-p'(z) + \frac{1}{y^q} \frac{\partial}{\partial y}\left(y^q\, \tau_{yz} \right) = 0 \tag{22}$$

$$\begin{aligned} \tau_{yz} &= \eta(\dot\gamma) \frac{\partial u}{\partial y} \\ \eta(\dot\gamma) &= 1 + \frac{Bn}{\dot\gamma}(1 - \exp(-M\dot\gamma)) \end{aligned} \tag{23}$$

3.1. Newtonian fluid

First, we find the analytical solution for a Newtonian fluid, i.e., for $Bn = 0$ and/or for $M = 0$. In this case, the apparent viscosity is constant, $\eta = 1$, and the shear stress is given by $\tau_{yz} = \partial u/\partial y$. Then, the momentum balance, Eq. (22), reduces to $0 = -p'(z) + \partial^2 u/\partial y^2$ for the channel, and to $0 = -y p'(z) + \partial(y\, \partial u/\partial y)/\partial y$ for the pipe, where hereafter a prime denotes differentiation with respect to z. Both equations can be integrated twice with respect to the vertical coordinate, y, and upon application of the boundary (Eq. (6)) and symmetry (Eq. (7)) conditions, the axial velocity component is derived. Plugging the solution into the total mass balance, Eq. (8), we find the unknown pressure gradient. Finally, the solution is completed by integrating the continuity equation, Eq. (21), with respect to the vertical coordinate and applying the no-penetration condition to find the transverse velocity component. Thus, for the channel, the solution for the field variables is:

$$\begin{aligned} u(y,z) &= \frac{3\left(h^2(z) - y^2\right)}{2h^3(z)} \\ v(y,z) &= \frac{3y\left(h^2(z) - y^2\right)h'(z)}{2h^4(z)} \\ p'(z) &= -\frac{3}{h^3(z)} \end{aligned} \tag{24}$$

Similarly, the solution for the pipe is:

$$\begin{aligned} u(y,z) &= \frac{4\left(h^2(z) - y^2\right)}{h^4(z)} \\ v(y,z) &= \frac{4y\left(h^2(z) - y^2\right)h'(z)}{h^5(z)} \\ p'(z) &= -\frac{16}{h^4(z)} \end{aligned} \tag{25}$$

As it can easily be confirmed from Eqs. (24) and (25), at any distance from the inlet plane, z, $\partial u/\partial y < 0$ and therefore the maximum axial velocity at any cross-section is observed at the midplane, $u(0,z) = 3/(2h(z))$ and $v(0,z) = 0$ for the channel, and at the axis of symmetry for

the pipe, $u(0,z) = 4/h^2(z)$ and $v(0,z) = 0$.

3.2. Bingham fluid

In ideal Bingham flows ($M \to \infty$), one needs to determine the yielded and unyielded regions of the flow domain, denoted respectively by

$$\Omega_{yielded} = \{(y,z) \parallel \sigma(z) < y \le h(z), 0 \le z \le 1\}$$

and

$$\Omega_{unyielded} = \{(y,z) \parallel 0 \le y \le \sigma(z), 0 \le z \le 1\}$$

where $\sigma = \sigma(z)$ is the position of the yield surface ($0 \le \sigma(z) < h(z)$). The latter is the locus of $\dot{\gamma}(\sigma(z),z) = 0$.

3.2.1. Channel flow

The governing equations in the yielded region are given by Eqs. (21)–(23) with $q = 0$ and without the exponential term in the formula for the apparent viscosity (Eq. (23b)). The shear stress is found by integrating Eq. (22) with respect to y and using Eq. (23) and the symmetry condition, Eq. (7b). This gives $\tau_{yz} = p'(z)\, y = -\dot{\gamma} - Bn$ which is integrated once more to give the velocity profile $u(y,z) = (y^2 - h^2(z))p'(z)/2 + Bn\,(y - h(z))$ in $\Omega_{yielded}$. The condition that determines the yield surface gives $\sigma(z) = -Bn/p'(z)$. Therefore, the axial velocity component in both regions ($\Omega_{yielded}$ and $\Omega_{unyielded}$) reads:

$$u = \begin{cases} \left(y^2 - h^2\right)p'/2 + Bn\,(y-h), & \sigma < y \le h \\ -\dfrac{(Bn + h\,p')^2}{2p'}, & 0 \le y \le \sigma \end{cases} \tag{26}$$

Eq. (26) is the same as Eq. (24) in Ref. [8] (with $y_w = h$, $y_y = \sigma$ and after a few manipulations).

Then, the unknown pressure gradient is found by plugging Eq. (26) into the total mass balance, Eq. (8), which after a little algebra, gives the third-order polynomial equation:

$$\Phi^3 - 3\left(\frac{1}{h^2} + \frac{Bn}{2}\right)\Phi^2 + \frac{Bn^3}{2} = 0 \tag{27}$$

where $\Phi(z) \equiv -p'(z)h(z) > 0$ has been used. From the definition of Φ and the solution for the yield surface, it is easily concluded that $\Phi(z) \ge Bn$ for any $z \in [0,1]$. Moreover, it can be confirmed that Eq. (27) has one positive and two negative real roots. For a straight channel with two parallel walls, $h(z) = 1$ and $p'(z) = -3$, which implies that $\Phi(h^2 = 1, Bn = 0) = 3$. Therefore, the relevant root of Eq. (27) is the one that satisfies $\lim_{Bn \to 0} \Phi = 3$ and is given by:

$$\Phi = \frac{1}{h^2} + \frac{Bn}{2} + \left(\frac{2}{h^2} + Bn\right)\cos\left[\frac{1}{3}\cos^{-1}\left(1 - \frac{2\left(h^2 Bn\right)^3}{\left(2 + h^2 Bn\right)^3}\right)\right] \tag{28}$$

For a straight channel, Eq. (28) reduces to the solution provided in Ref. [13] (see Eq. (2.54) with $C = \Phi$ and $\tau_y = Bn$). Also, an upper bound for Φ can be found from Eq. (28), i.e. $\Phi \le 3(1/h^2 + Bn/2)$. Moreover, by taking into account that $\Phi(z) \ge Bn$, one finds the range for $\Phi \equiv -hp'$ valid for any Bingham number $Bn \ge 0$ and positive shape function $h > 0$:

$$Bn \le \Phi \le 3\left(\frac{1}{h^2} + \frac{Bn}{2}\right) \tag{29}$$

From Eq. (28) one can trivially confirm that as $Bn \to 0$, $\Phi \to 3/h^2$ as it should (see the Newtonian solution in subsection 3.1). Moreover, the lower limit in Eq. (29) is approached for small values of the Bingham number, while the upper limit is approached as the Bingham number becomes very large (more details are provided in Appendix A). Finally, for a straight channel, namely for $h = 1$, $\Phi \equiv -p'$ and Eq. (28) reduces to:

$$\Phi = 1 + \frac{Bn}{2} + (2 + Bn)\cos\left[\frac{1}{3}\cos^{-1}\left(1 - \frac{2Bn^3}{(2 + Bn)^3}\right)\right] \tag{30}$$

Note that if we set $\xi = \Phi/Bn$ (i.e., $p' = -Bn\,\xi/h$) and $Bn = B^*/h^2$, and substitute in Eq. (27), we obtain the Buckingham equation (see Eq. (27) in Ref. [8]):

$$2\xi^3 - 3\left(1 + \frac{2}{B^*}\right)\xi^2 + 1 = 0 \tag{31}$$

where $\xi = \xi(B^*)$, and now the relevant root of Eq. (31) is that with $\xi > 1$. Therefore, Eqs. (27) and (31) are equivalent for any $Bn > 0$, albeit we prefer Eq. (27) because it is valid even for $Bn = 0$. It is also worth reporting the analytical solution for ξ:

$$\xi = \frac{1}{2} + \frac{1}{B^*} + \left(\frac{2}{B^*} + 1\right)\cos\left[\frac{1}{3}cos^{-1}\left(1 - \frac{2B^{*3}}{(2 + B^*)^3}\right)\right] \tag{32}$$

Finally, by integrating the continuity equation, Eq. (21), we find for the transverse velocity component:

$$v = \begin{cases} -\dfrac{p''}{6}(y+2h)(y-h)^2 + (p'h + Bn)(y-h)h', & \sigma < y \le h \\ -\dfrac{(Bn + hp')^2}{p'}\left(\dfrac{(Bn - 2hp')p''}{6p'^2} - h'\right), & 0 \le y \le \sigma \end{cases} \tag{33}$$

where $\sigma = -Bn/p'$, $p' = -\Phi/h$ and $p'' = -(\Phi/h)'$. Notice that $v(y = 0, z) \ne 0$ which is a consequence of the fact that at the lubrication limit, the condition of a zero transverse velocity cannot be satisfied.

From Eq. (26), one can easily confirm that $\partial u/\partial y < 0$ in $\Omega_{yielded}$. Also, for $Bn \to 0$, $\sigma(z) \to 0$ (i.e., no unyielded region appears in the flow) and $p' \to -3/h^3$. In this case, Eqs. (26) and (33) reduce to the corresponding formulas given in Eq. (24) for a Newtonian fluid.

3.2.2. Pipe flow

The governing equations are given by Eqs. (21)–(23) with $q = 1$ and in absence of the exponential term in the formula for the apparent viscosity (Eq. (23b)). In the yielded region, the shear stress is found by integrating Eq. (22) with respect to y and using Eq. (23) and the symmetry condition, Eq. (7). This gives $\tau_{yz} = p'(z)\, y/2 = -\dot{\gamma} - Bn$ which is integrated once more to give the velocity profile $u(y,z) = (y^2 - h^2(z))\, p'(z)/4 + Bn\,(y - h(z))$ in $\Omega_{yielded}$. The condition that determines the yield surface gives $\sigma(z) = -2Bn/p'(z)$. Thus, the axial velocity component in both regions is:

$$u = \begin{cases} \dfrac{1}{4}\left(y^2 - h^2\right)p' + Bn\,(y-h), & \sigma \le y \le h \\ -\dfrac{(Bn + hp'/2)^2}{p'}, & 0 \le y \le \sigma \end{cases} \tag{34}$$

The unknown pressure gradient is found by plugging u into the total mass balance, Eq. (8) with $q = 1$, which after a little algebra, gives the fourth-order polynomial equation:

$$\Phi^4 - 4\left(\frac{Bn}{3} + \frac{2}{h^3}\right)\Phi^3 + \frac{Bn^4}{3} = 0 \tag{35}$$

where $\Phi = -hp'/2$. For a straight pipe ($h = 1$) and defining $\widehat{\Phi} = 1/\Phi$, Eq. (35) transforms to the Buckingham-Reiner equation [26] (see also Eq. (2.51) in [13] with $C = \Phi$ and $\tau_y = Bn$). Eq. (35) shows that Φ depends on Bn and h^3. It has four roots from which only one reduces to the correct limit as $Bn \to 0$ for a straight pipe, namely to $\Phi \to 8$. This root can be compactly printed if we set $K \equiv 4(Bn/3 + 2/h^3) > 0$ and $C \equiv Bn^4/3 >$

0 as follows:

$$\Phi = \frac{K}{4} + \frac{1}{2}\sqrt{\frac{K^2}{4} + X} + \frac{1}{2}\sqrt{\frac{K^2}{2} - X + \frac{K^3}{4\sqrt{\frac{K^2}{4} + X}}},$$

$$X \equiv \frac{4(2/3)^{1/3} C}{\left(9C K^2 + \sqrt{81C^2K^4 - 768C^3}\right)^{1/3}} + \frac{\left(9C K^2 + \sqrt{81C^2K^4 - 768C^3}\right)^{1/3}}{2^{1/3}3^{2/3}} \tag{36}$$

The solution for the field variables is completed by integrating Eq. (21) with respect to y to find the transverse velocity component:

$$v = \begin{cases} -\frac{p''}{16}y^3 + \frac{4Bnh' + (h^2)'p' + h^2p''}{8}y - \frac{h^2(8Bnh' + 2(h^2)' + h^2p'')}{16y}, & \sigma \le y \le h \\ \frac{1}{32Bnp'}\left(\frac{((hp')^2 - (2Bn)^2)^2 p''}{p'^2} - (2Bn - hp')\left(Bn + \frac{hp'}{2}\right)^2 h'\right), & 0 \le y \le \sigma \end{cases} \tag{37}$$

As previously mentioned for the channel, $v(y = 0, z) \neq 0$ due to the lubrication approximation.

For $Bn \to 0$ the yield surface approaches the axis of symmetry, $\sigma(z) \to 0$, i.e., no unyielded region appears in the flow. In this case, the last term in the formula for v is well-defined at $y = 0$ provided that the numerator is zero. This implies that $p' = c/h^4$ where c is constant. With the aid of the total mass balance, we find that $c = -16$, and thus $p' \to -16/h^4$ as $Bn \to 0$. Thus, Eqs. (34) and (37) reduce to the corresponding formulas for a Newtonian fluid given in Eq. (25).

3.3. Papanastasiou fluid

Here, we derive the analytical solution for the regularized Papanastasiou model, i.e., for finite values of the exponential parameter M. For large values of M, the Papanastasiou model approaches the ideal Bingham model with the advantage that no yield surface is needed to be found, namely the material flows over the entire domain Ω. Thus, in the following subsections, Eqs. (21)–(23) are solved with $q = 0$ for the channel, and with $q = 1$ for the pipe, on Ω.

3.3.1. Channel flow

Integrating Eq. (22) with respect to y, using the symmetry of the flow field about the midplane, the fact that $\dot{\gamma} = |\partial u/\partial y| = -\partial u/\partial y > 0$ for $0 < y < h(z)$, as well as Eq. (23), we find the following expression for $\dot{\gamma}$:

$$\tau_{yz} = p'(z)\, y = -\dot{\gamma} - Bn(1 - \exp(-M\dot{\gamma})) \tag{38}$$

Notice that Eq. (38) imposes the restriction:

$$p'(z)\, y + \dot{\gamma} + Bn \ge 0 \tag{39}$$

where the equality holds only when $M \to \infty$. Eq. (39) must be checked a-posteriori to confirm the validity of the solution. Following You et al. [16], Eq. (38) is rearranged, multiplied by $M\exp(M(p'(z)\, y + \dot{\gamma} + Bn))$ and simplified suitably, to yield the solution for $\dot{\gamma}$:

$$\dot{\gamma} = -p'(z)\, y - Bn + \frac{1}{M} \underbrace{W(M\, Bn \exp(M(p'(z)\, y + Bn))}_{f(y,z)} \tag{40}$$

In Eq. (40) W is the Lambert W special function [14,15] which gives the principal root for z of the transcendental equation $z e^z = x$; the latter has two real roots for $-1/e \le x < 0$ and one real non-negative and strictly increasing root for $x \ge 0$ ($W(x) = 0 \Leftrightarrow x = 0$). Since M, Bn and $f(y, z)$ are all non-negative, hereafter Wwill be representing the primary branch of the Lambert function. Sometimes, in modern mathematical software and other applications, the "product-logarithm function" is used instead. In fluid mechanics, application of the Lambert W function to steady shearing flows of the Papanastasiou model can be found in Ref. [16], to steady flow of an exponential Phan-Thien & Tanner fluid in a straight channel in Ref. [17], as well as to other simple flows Eq. (34) is the same with Eq. (24) in Ref. [18]; note that all the flow problems considered in Refs [15–18] are unidirectional or homogeneous. For more details about the Lambert function, the interested reader is referred to Refs [6,14,15].

Notice that if we substitute the solution for $\dot{\gamma}$ into the inequality (39) reduces to the trivial $W(f(y, z)) \ge 0$ which holds for any value of y and z because $f(y, z) > 0$ and due to the properties of the Lambert function. Eq. (40) can be used in conjunction with Eq. (8) to find the unknown pressure gradient, $p'(z)$. First, we integrate by parts Eq. (8) and apply the no-slip condition at the upper wall, Eq. (6a), to find $\int_0^{h(z)} y\dot{\gamma}\, dy = 1$. Then, substituting Eq. (40) into the latter and performing the integration with respect to y from the midplane ($y = 0$) to the upper wall ($y = h(z)$), gives:

$$-\frac{1}{3}p'(z)\, h^3(z) - \frac{Bn}{2}\, h^2(z) + \underbrace{\frac{1}{M}\int_0^{h(z)} y\, W(f(y, z))dy}_{I(z)} = 1 \tag{41}$$

Using suitable properties of the Lambert function and denoting with $w = w(z)$ the Lambert function off$(y = h(z), z)$:

$$w(z) \equiv W(f(h(z), z)) = W(M\, Bn \exp(M(p'(z)h(z) + Bn)) \tag{42}$$

the integral $I(z)$ in Eq. (41) is found as follows:

$$I = \frac{1}{2M^2p'^2}\left[-\frac{w^3}{3M} + \frac{(M\, h\, p' - 3)w^2}{2M} + \frac{2(M\, h\, p' - 1)w}{M} + Bn(12 + Bn\, M(9 + 2M\, Bn))\right] \tag{43}$$

In Eq. (43), the explicit dependence of p' and h on z has been omitted. Substituting Eq. (43) into Eq. (41), multiplying the resulting equation by p'^2, and setting $\Phi(z) \equiv -p'(z)\, h(z) > 0$ gives:

$$\Phi^3 - 3\left(\frac{1}{h^2} + \frac{Bn}{2}\right)\Phi^2 - \frac{3w(w+2)}{2M^2}\Phi - \frac{3w}{M^3}\left(1 + \frac{3w}{4} + \frac{w^2}{6}\right) + \frac{3Bn}{M^2} + \frac{9Bn^2}{4M} + \frac{Bn^3}{2} = 0 \tag{44}$$

The above equation is a strongly non-linear algebraic equation for $\Phi = \Phi(z)$. Solving Eq. (44) numerically with a Newton scheme at a set of grid points along the axial coordinate z (where $z \in [0, 1]$) gives Φ and in turn $p' = -\Phi/h$. Note that if we start the Newton scheme with the corresponding analytical solution for the Bingham fluid, i.e., with Eq. (28), the iterative procedure at each grid point converges and terminates after a couple of iterations.

The axial velocity component, $u = u(y, z)$, can be found by integrating Eq. (40) with respect to the transverse coordinate between y and h(z) and applying the no-slip condition at the wall:

$$u(y, z) = p'(z)\, \frac{y^2 - h^2(z)}{2} + Bn\, (y - h(z)) + I_u(y, z) \tag{45}$$

where

$$I_u(y, z) = \frac{1}{M}\int_y^{h(z)} W(f(\tilde{y}, z))d\tilde{y} \tag{46}$$

Note that if we plug the above velocity profile into the total mass bal-

ance, i.e., to Eq. (8) with $q = 0$, we get Eq. (41), as expected. In Eq. (46), $I_u(y,z)$ can be evaluated in terms of $W(f(y,z))$ and $w \equiv W(f(h(z),z))$ using properties of the Lambert function:

$$I_u(y,z) = \frac{1}{M^2 p'(z)} \left\{ w(z)\left(1+\frac{w(z)}{2}\right) - W(f(y,z))\left(1+\frac{W(f(y,z))}{2}\right)\right\} \tag{47}$$

Finally, the solution is completed by calculating the transverse velocity component, $v = v(y,z)$. This is achieved by integrating the continuity equation (Eq. (21)) with respect to y. Applying the no-slip and no-penetration conditions, and Leibniz's rule for integrals gives $v(y,z) = \frac{\partial}{\partial z}\int_y^{h(z)} u(s,z)\,ds$. Substituting u as given in Eq. (45), performing the integration/differentiation, and using properties of the Lambert function gives:

$$v(y,z) = \left(-\frac{y^3}{6}+\frac{h^2(z)y}{2} - \frac{h^3(z)}{3}\right)p''(z) + (p'(z)h(z)+Bn)(y-h(z))\,h'(z) + I_v(y,z) \tag{48}$$

where

$$I_v(y,z) = \frac{\partial}{\partial z}\left[\int_y^h I_u(\tilde{y},z)d\tilde{y}\right] = \frac{\partial}{\partial z}(F(h,z)-F(y,z)) \tag{49}$$

and

$$F(y,z) = \frac{-W}{M^3 p'^2}\left(1+\frac{3W}{4}+\frac{W^2}{6}\right) + \frac{y\,w}{M^2 p'}\left(1+\frac{w}{2}\right) \tag{50}$$

In the above equation $W \equiv W(f(y,z))$ and $w \equiv W(f(h(z),z))$ have been used for brevity; see Eqs. (40) and (42), respectively.

The standard limiting cases are considered first. As the Bingham number goes to zero, and assuming finite values of the Papanastasiou parameter (i.e., for $Bn \to 0$ and $M = O(1)$), we see that $W \to 0$ and Eq. (44) gives $\Phi \to 3/h^2$ from which $p' \to -3/h^3$ follows. The same holds for $M \to 0$ and $Bn = O(1)$. Thus, in both cases, the Newtonian solution is recovered. Finally, when the exponential parameter M becomes very large, the regularized Papanastasiou model must reduce to the ideal yield-stress Bigham model. Indeed, in this case, (i.e., for $M \to \infty$ and $Bn = O(1)$), we find that $w \to 0$ and Eq. (44) reduces to Eq. (27).

3.3.2. Pipe flow

Integrating Eq. (22) with respect to y, using that the flow is axisymmetric, the fact that $\dot{\gamma} = |\partial u/\partial y| = -\partial u/\partial y > 0$ over the entire domain Ω, as well as Eq. (23), we find:

$$\tau_{yz} = p'(z)\,\frac{y}{2} = -\dot{\gamma} - Bn(1-\exp(-M\dot{\gamma})) \tag{51}$$

Eq. (51) imposes the restriction:

$$p'(z)\,y/2 + \dot{\gamma} + Bn \geq 0 \tag{52}$$

where the equality holds only when $M \to \infty$, and as for the channel flow, Eq. (52) must be used a-posteriori to check the validity of the solution. Following You et al. [16], Eq. (51) is rearranged, multiplied by $M\exp(M(p'(z)\,y/2+\dot{\gamma}+Bn))$ and simplified suitably to yield the solution for the shear-rate:

$$\dot{\gamma} = -p'(z)\,\frac{y}{2} - Bn + \frac{1}{M} W\underbrace{(M\,Bn\,\exp(M(p'(z)\,y/2+Bn))}_{f(y,z)} \tag{53}$$

Noting that $f(y,z) > 0$, and substituting the solution for $\dot{\gamma}$ into inequality (52) gives the trivial $W(f(y,z)) \geq 0$ which holds for any value of y and z because of the properties of the Lambert function.

Eq. (53) is used in conjunction with Eq. (8) to find the unknown pressure gradient, $p'(z)$. First, we integrate by parts Eq. (8) and apply the no-slip condition at the upper wall to find $\int_0^{h(z)} y^2\,\dot{\gamma}\,dy = 2$. Then, by substituting Eq. (53) into the latter, and performing the integration with respect to y from the axis of symmetry ($y = 0$) to the wall ($y = h(z)$), gives:

$$-\frac{1}{8}p'(z)\,h^4(z) - \frac{1}{3}Bn\,h^3(z) + \underbrace{\frac{1}{M}\int_0^{h(z)} y^2\,W(f(y,z))dy}_{I(z)} = 2 \tag{54}$$

Using properties of the Lambert function and denoting with $w = w(z)$ the value of W function at $f(y = h(z),z)$, i.e.:

$$w(z) \equiv W(f(h(z),z)) = W(M\,Bn\,\exp(M(p'(z)h(z)/2+Bn)) \tag{55}$$

we find the integral $I(z)$ in Eq. (54) in terms of W and w. Then, we set $\Phi(z) \equiv -p'(z)\,h(z)/2 > 0$, rearrange the resulting equation and upon simplification, we derive the strongly non-linear algebraic equation for Φ:

$$\Phi^4 - 4\Phi^3\left(\frac{Bn}{3}+\frac{2}{h^3}\right) - \frac{2W(2+W)}{M^2}\Phi^2 - \frac{2W(12+9W+2W^2)}{3M^3}\Phi + \frac{-W(72+63W+22W^2+3W^3)}{9M^4} + \frac{Bn}{M}\left(\frac{8}{M^2}+\frac{7Bn}{M}+\frac{22Bn^2}{9}\right) + \frac{Bn^4}{3} = 0 \tag{56}$$

The limiting (Newtonian and Bingham) cases follow. As the Bigham number goes to zero, $Bn \to 0$, and assuming finite values of the exponential parameter, $M = O(1)$, we see that $W \to 0$. Thus, Eq. (56) gives $\Phi = 8/h^3$ from which $p' = -16/h^4$ follows. The same holds when $M \to 0$ and $Bn = O(1)$. When $M \to \infty$ and $Bn = O(1)$, we see that $W \to 0$ too, and Eq. (56) reduces to Eq. (35), namely the equation for the Bingham fluid is recovered.

The axial velocity component, $u = u(y,z)$, can be found by integrating Eq. (53) with respect to y between y and h(z) and applying the no-slip condition at the wall:

$$u(y,z) = p'(z)\,\frac{y^2-h^2(z)}{4} + Bn\,(y-h(z)) + I_u(y,z) \tag{57}$$

where

$$I_u(y,z) = \frac{1}{M}\int_y^{h(z)} W(f(s,z))ds \tag{58}$$

Note that if we plug the above velocity profile into the total mass balance, i.e., to Eq. (8), we find Eq. (54), as it should. The integral in Eq. (58) can be evaluated in terms of $W(f(y,z))$ and $W(f(h(z),z)) \equiv w(z)$:

$$I_u(y,z) = \frac{1}{M^2 p'(z)}\left\{w(z)\left(1+\frac{w(z)}{2}\right) - W(f(y,z))\left(1+\frac{W(f(y,z))}{2}\right)\right\} \tag{59}$$

Finally, the solution is completed by calculating the radial velocity component, $v = v(y,z)$, with the aid of the continuity equation (Eq. (21) with $q = 1$) and using the no-slip and no-penetration conditions:

$$v(y,z) = \frac{1}{y}\frac{\partial}{\partial z}\int_y^{h(z)} (s\,u(s,z))\,ds \tag{60}$$

4. Pressure drop

The most interesting quantity for this type of flows is the pressure drop required to maintain the constant volumetric flowrate through the duct [19,20]. The analysis for the channel and the pipe is presented here

separately, by considering two standard cases for the shape function that describes the wall(s) of the duct.

4.1. Channel flow

For this geometry, the average pressure drop, $\Delta\bar{p} > 0$, is generally given as:

$$\Delta\bar{p} = \int_{-h(0)}^{h(0)} p(y, z=0)dy - \int_{-h(1)}^{h(1)} p(y, z=1)dy = 2(h(0)p(z=0) - h(1)p(z=1)) \tag{61}$$

where the second equality results from the fact that at the classic lubrication limit (i.e., for $\varepsilon \to 0$) the total pressure is independent of the vertical direction, y. Recalling that the shape function $h = h(z)$ has been scaled by $h_0^* \equiv h^*(z^*=0)$ which implies that $h(z=0) = 1$, arbitrary setting the datum pressure $p(z=1) = 0$ and using that $p(1) - p(0) = \int_0^1 p'(z)dz$, Eq. (61) reduces to the following general expression:

$$\Delta\bar{p} = -2\int_0^1 p'(z)dz = 2\int_0^1 (\Phi(z)/h(z))dz \tag{62}$$

where in the second equality p' has been expressed by means of Φ. Hereafter, we will be using the subscripts *N, B,* and *P* in $\Delta\bar{p}$ to denote the solution for the Newtonian, ideal Bingham and regularized Papanastasiou fluids, respectively. As discussed in Section 3, analytical expressions for the pressure gradient $p'(z)$ can be obtained analytically only for the Newtonian and ideal Bingham fluids; see Eqs. (24c) and (28), respectively. In the Newtonian case, $p'(z)$ is substituted in Eq. (62) and the pressure drop is found as:

$$\Delta\bar{p}_N = 6\int_0^1 h^{-3}(z)dz \tag{63}$$

For the ideal Bingham fluid, Eq. (62) and the solution for Φ given by Eq. (28), give:

$$\Delta\bar{p}_B = \underbrace{2\int_0^1 \frac{dz}{h^3(z)}}_{\Delta\bar{p}_N/3} + Bn\int_0^1 \frac{dz}{h(z)} + 2\int_0^1 \left(\frac{2}{h^3(z)} + \frac{Bn}{h(z)}\right) \times cos\left[\frac{1}{3}cos^{-1}\left(1 - \frac{2\left(h^2(z)Bn\right)^3}{\left(2 + h^2(z)Bn\right)^3}\right)\right]dz \tag{64}$$

It is also interesting to note that due to Eqs. (28) and (64), the following bounds for $\Delta\bar{p}_B$ can be easily deduced:

$$2Bn\int_0^1 \frac{dz}{h(z)} \le \Delta\bar{p}_B \le \Delta\bar{p}_N + 3Bn\int_0^1 \frac{dz}{h(z)} \tag{65}$$

For the Papanastasiou model, the pressure drop $\Delta\bar{p}_P$ is calculated numerically based on the general formula in terms of Φ, Eq. (63), where Φ is the solution of Eq. (44).

For fully periodic undulating ducts (channels or pipes), a typical shape function is:

$$h(z) = 1 - \frac{\lambda}{2}(1 - \cos(2\pi k\, z)) \tag{66}$$

where λ is the amplitude of the undulation and k (a positive integer) is the number of undulations. For $0 < \lambda < 1$ a channel with k-restrictions is described, while for $\lambda < 0$ the shape function describes a channel with k-bumps. For $\lambda = 0$ one gets a straight channel with two parallel walls. Plugging Eq. (66) into Eq. (63) and performing the integration, gives the pressure drop for a Newtonian fluid:

$$\Delta\bar{p}_N = \frac{3\left(8 - 8\lambda + 3\lambda^2\right)}{4(1-\lambda)^{5/2}} \tag{67}$$

Notice that the wavenumber k does not appear in the formula for $\Delta\bar{p}_N$ [20]. Similarly, for the ideal Bingham fluid, one finds:

$$\Delta\bar{p}_B = \frac{8 - 8\lambda + 3\lambda^2}{4(1-\lambda)^{5/2}} + \frac{Bn}{\sqrt{1-\lambda}} + 2\int_0^1 \left(\frac{2}{h^3(z)} + \frac{Bn}{h(z)}\right)\cos(Y(z))dz, \qquad Y(z) = \frac{1}{3}\cos^{-1}\left(1 - \frac{2\left(h^2(z)Bn\right)^3}{\left(2 + h^2(z)Bn\right)^3}\right) \tag{68}$$

The integral term in Eq. (68) cannot be found analytically for $Bn > 0$. Also, as mentioned above for $\Delta\bar{p}_N$, the wavenumber k does not affect $\Delta\bar{p}_B$ and $\Delta\bar{p}_P$.

For linearly converging/diverging channels, the shape of the walls is described by the linear function:

$$h(z) = 1 + \delta h\, z \tag{69}$$

where $\delta h \equiv h(z=1) - h(z=0) = h_f - 1$ is the amplitude of the wall variation with h_f being the half-height of the channel at the outlet plane. For $-1 < \delta h < 0$ (or $0 < h_f < 1$) one gets a converging channel, for $\delta h > 0$ (or $h_f > 1$) a diverging channel, and for $\delta h = 0$ (or $h_f = 1$) a straight channel with two parallel walls.

Substituting Eq. (69) in Eq. (63) and performing the integration, gives:

$$\Delta\bar{p}_N = \frac{3(2 + \delta h)}{(1 + \delta h)^2} \tag{70}$$

Similarly, substituting Eq. (69) into the first two terms in Eq. (68) gives:

$$\Delta\bar{p}_B = \frac{2 + \delta h}{(1 + \delta h)^2} + Bn\frac{\ln(1 + \delta h)}{\delta h} + 2\int_0^1 \left(\frac{2}{h^3(z)} + \frac{Bn}{h(z)}\right)\cos(Y(z))dz \tag{71}$$

for the ideal Bingham fluid, where $Y(z)$ is given in Eq. (68) and the last term in Eq. (71) cannot be found analytically.

4.2. Pipe flow

For this geometry, the analysis is quite similar to that for the channel flow and thus most of the details are omitted. The average pressure drop is:

$$\Delta\bar{p} = \int_0^{h(0)} p(y, z=0)ydy - \int_0^{h(1)} p(y, z=1)ydy = \frac{1}{2}\left(h^2(0)p(z=0) - h^2(1)p(z=1)\right) \tag{72}$$

where the second equality results from the fact that at the classic lubrication limit, the total pressure is independent of the radial direction, y.

Since $h(0) = 1$ and $p(z=1) = 0$ can be set arbitrarily, Eq. (72) reduces to:

$$\Delta\bar{p} = -\frac{1}{2}\int_0^1 p'(z)dz = \int_0^1 (\Phi(z)/h(z))dz \tag{73}$$

where in the second equalityp' has been expressed in terms of Φ. For a Newtonian fluid, Eq. (73) gives:

$$\Delta\bar{p}_N = 8\int_0^1 h^{-4}(z)dz \tag{74}$$

Using the shape function for the undulating pipe (Eq. (66)) into Eq. (74) gives:

$$\Delta\bar{p}_N = \frac{(2-\lambda)\left(8-8\lambda+5\lambda^2\right)}{2(1-\lambda)^{7/2}} \tag{75}$$

Similarly, using the linear shape function (Eq. (69)) into Eq. (74) gives:

$$\Delta\bar{p}_N = \frac{8\left(3+3\delta h+\delta h^2\right)}{3(1+\delta h)^3} \tag{76}$$

As expected, the flows become singular when $\lambda \to 1^-$ and when $\delta h \to -1^+$ (the pressure drop diverges to infinity) because the area of the cross-section becomes zero and the flow through the duct is not possible. Convenient analytical formulas for $\Delta\bar{p}_B$ and $\Delta\bar{p}_P$ could not be found.

5. Results and discussion

First, we present the results for the normalized pressure drop, $\Delta\bar{p}_N/\Delta\bar{p}_N(\lambda=0)$, in Fig. 2, for both configurations, where $\Delta\bar{p}_N(\lambda=0)=6$ for the channel and $\Delta\bar{p}_N(\lambda=0)=8$ for the pipe. Fig. 2a shows the normalized pressure drop as function of the amplitude of the undulation, λ, in the range $-1 \le \lambda < 0.9$, while Fig. 2b shows the corresponding results as function of the amplitude of the wall variation, δh, in the range $-0.9 < \delta h < 1$. Notice, that the results for the pipe are very similar with the results for the channel. The same holds for the ideal Bingham and regularized Papanastasiou fluids. Thus, in the remaining of this section, most of the results will be presented for the channel flow only.

For the ideal Bingham flow in a symmetric channel, the results for the pressure drop normalized with the pressure drop for a straight duct as function of the Bingham number are presented in Fig. 3. Fig. 3a shows $\Delta\bar{p}_B/\Delta\bar{p}_B(\lambda=0)$ in the undulating case with λ=0.25, 0.50 and 0.75, while Fig. 3b shows $\Delta\bar{p}_B/\Delta\bar{p}_B(\delta h=0)$ for a linearly varying channel with δ_h=-0.9 (converging), 0 (straight) and 0.9 (diverging). The results are based on the exact solution, Eq. (68), the asymptotic formulas at small *Bn* (see Eqs. (A6) and (A8) in Appendix A) as well as on the two-point approximate formula, Eq. (A3), which is reported in Appendix A too. In all cases, an increase of the pressure drop with the increase of Bingham number is observed. It is interesting to note, and not intuitively expected, that the increase is faster the closer the channel to a straight one. We also see excellent agreement between the exact solutions and the asymptotic solutions at small Bingham numbers, although over a range that shrinks as the amplitude of the wall (or the amplitude of the wall variation in the linear case) decreases. On the contrary, the agreement of two-point approximate formula (A3) is great over the entire range of the Bingham number shown clearly showing that the analysis performed based on two limits (*Bn*→0 and *Bn*→∞) is successful and suitable to be used for this type of flows.

The effect of the exponential parameter, *M*, of the Papanastasiou model is investigated in Fig. 4 for *Bn*=1. One is reminded here that as the exponential parameter goes to infinity, the Papanastasiou model theoretically approaches the ideal Bingham fluid (and therefore $\Delta\bar{p}_P(M\to\infty) \equiv \Delta\bar{p}_B$). However, the limiting behavior of the regularized model is established quickly at finite values of *M*. Indeed, the results for $\Delta\bar{p}/\Delta\bar{p}(M\to\infty) \equiv \Delta\bar{p}_P/\Delta\bar{p}_B$ which are presented as function of λ over an extended range, show that when $M = 10$ the asymptotic behavior of the solution at infinity is very well approximated over the entire range of the amplitude of the undulation. Thus, there is no need to go to higher values of the exponential parameter to simulate the ideal Bingham model. We also emphasize here that for $M > 10$ our calculations occasionally indicate loss of accuracy (terms like $W(MBn\exp(-M\dot{\gamma}))$ are too small to be represented accurately as normalized machine numbers even in modern computers causing underflow errors). Hence, $M = 10$ is used in all the results that are presented and discussed in the remaining of this section.

In Fig. 5, the pressure drop $\Delta\bar{p}$ normalized with the pressure drop for a straight duct, $\Delta\bar{p}(\lambda=0)$, is presented for *Bn*=0.5, 1.0 and 2.0. In particular, Fig. 5a shows $\Delta\bar{p}/\Delta\bar{p}(\lambda=0)$ as function of λ, and Fig. 5b shows $\Delta\bar{p}/\Delta\bar{p}(\delta h=0)$ as function of δh. As expected, the pressure drop diverges as λ approaches unity, and as δhapproaches minus one. In both cases a monotonic variation of the normalized pressure drop is observed. It is also seen that the increase of the Bingham number has a minor effect on $\Delta\bar{p}/\Delta\bar{p}(\lambda=0)$; a small decrease is predicted for a channel with restrictions (i.e. for $0 < \lambda < 1$), and a small increase for a channel with bumps (i.e. for $\lambda < 0$). It should be noted that the increase is larger the smaller the amplitude of the undulation. Similar observations apply for the linearly diverging/converging channel.

The effect of the Bingham number on the normalized pressure drop $\Delta\bar{p}/\Delta\bar{p}_N$ (where $\Delta\bar{p}_N \equiv \Delta\bar{p}(Bn=0)$ is the corresponding pressure drop for a Newtonian fluid) is systematically investigated in Fig. 6 for λ=0.25, 0.50 and 0.75. It is seen that the normalized pressure drop increases roughly linearly with the Bingham number. Also, as previously seen in Fig. 3, the slope decreases as the amplitude of the undulation increases. However, this is because the increase of the amplitude of the undulation causes larger shear rates, and thus the material yields everywhere in the duct. We also mention that the results for the ideal Bingham (dashed lines in Figure) essentially coincide with their counterparts for the Papanastasiou fluid. Once again, this clearly indicates that with $M = 10$

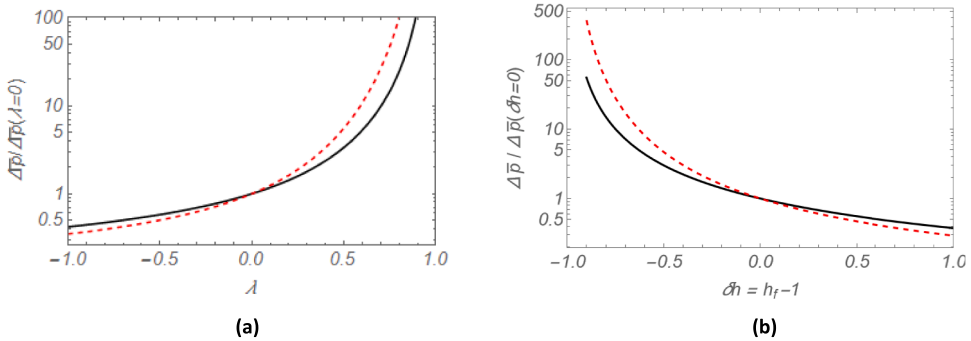

Fig. 2. Normalized average pressure drop for Newtonian flow. (a) as function of the amplitude of the undulation in a channel (black solid line) and in a pipe (red dashed line); (b) as function of the wall variation for linearly converging (-1<δ_h<0) and linearly diverging (δ_h>0) channel (black solid line) or pipe (red dashed line). (For interpretation of the references to colour in this figure legend, the reader is referred to the web version of this article.)

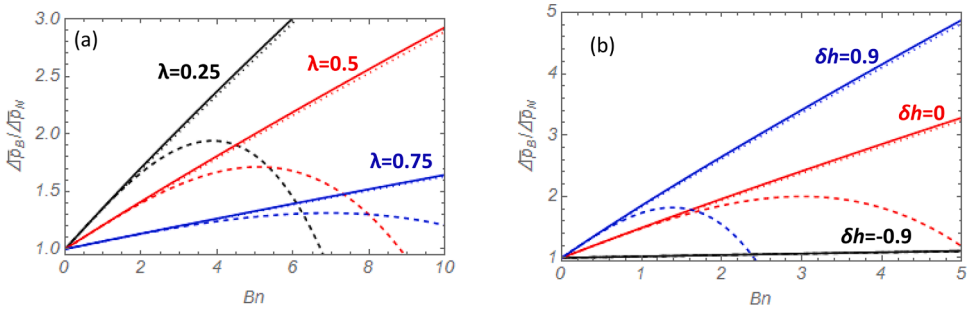

Fig. 3. Normalized pressure drop for the ideal Bingham flow in a symmetric channel as a function of the Bingham number computed using the exact analytical solution (Eq. (68), solid), asymptotic results at small Bigham numbers (Eqs (A6) and (A7), dashed), and the two-point Padé formula (see Eq.(A3), dotted): (a) undulating wall with λ=0.25, 0.5 and 0.75; (b) linearly-varying wall with λ_h=-0.9, 0, and 0.9.

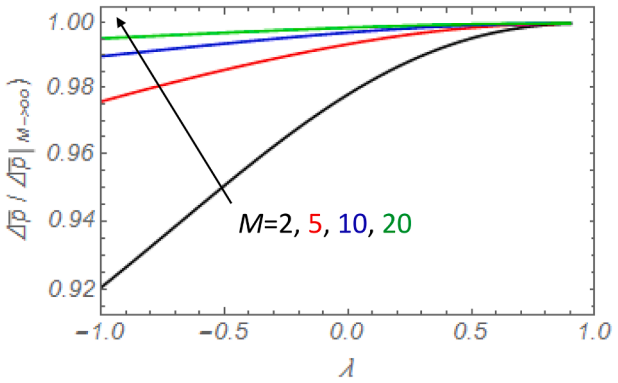

Fig. 4. The effect of the regularization parameter M (Papanastasiou fluid) on the normalized pressure drop for a symmetric channel as function of the amplitude of the undulation; Bn=1.

the limiting behavior of the Papanastasiou fluid at $M\to\infty$ is very well approximated.

Contours for the axial and vertical velocity components are shown in Fig. 7 for an undulating symmetric channel with λ=0.5 and $k = 1$. The Newtonian, ideal Bingham, and regularized Papanastasiou contours for Bn=2 and $M = 10$ are depicted at the top, middle and bottom panels, respectively. We observe that the largest values of the axial velocity are observed for a Newtonian fluid, while the contours for the Bingham and Papanastasiou fluids are almost identical; thus, the Pananastasiou model approximates very well the ideal Bingham fluid. Notice however, that the transverse velocity contours of the Papanastasiou fluid are very similar to the Newtonian ones. Interestingly, the limiting behavior of the Papanastasiou model for the transverse velocity component is approached much slower than the axial velocity and the pressure gradient. This is demonstrated clearly in Fig. 8, where the distributions of $u(x, y_0(x))$ and $v(x, y_0(x))$ are plotted, where the curve $y_0(x) = 0.1\,h(x)$ is close to the midplane. The axial velocity profiles for the Bingham and Papanastasiou fluids are almost indistinguishable, and the same holds for the transverse velocity profiles for the Newtonian and Papanastasiou fluids.

The maximum axial velocity as function of the distance from the inlet plane for a symmetric undulating channel with λ=0.5 and three undulations ($k = 3$) is presented in Fig. 9; the Bingham number is Bn=0.5 and $M = 10$. For all the models used in this work, $\partial u/\partial y < 0$ for any $0 \le y \le h(z)$ and any distance from the inlet plane; this implies that the maximum velocity is observed always at the midplane. We see that as the channel contracts the maximum velocity increases and vice versa, as

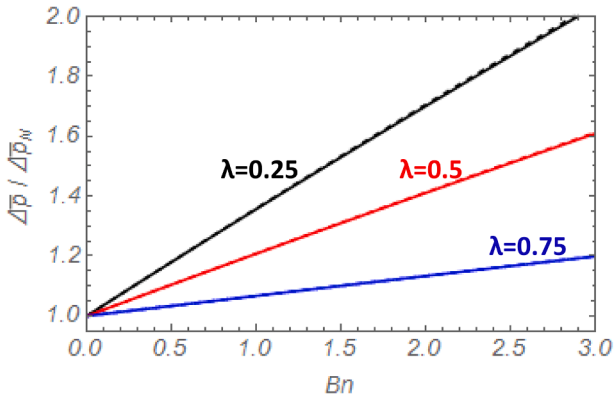

Fig. 6. Normalized pressure drops (solid lines) for the flow of a Papanastasiou fluid with $M = 10$ in an undulating symmetric channel with $k = 1$, as function of the Bingham number for various values of the amplitude of undulation λ. The hard-to-see dashed lines are their counterparts for an ideal Bingham fluid.

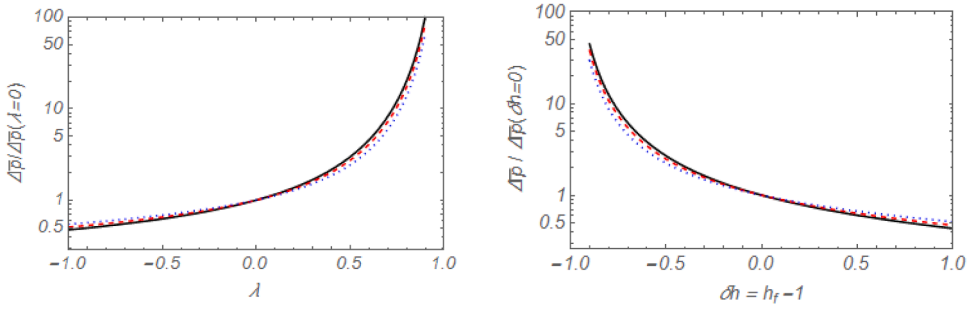

Fig. 5. Normalized pressure drop for the flow of a Papanastasiou fluid ($M = 10$) in a symmetric channel for Bn=0.5 (solid), 1 (dashed), and 2 (dotted) with (a) an undulating wall ($k = 1$), as a function of the amplitude of the undulation (b) a linearly varying wall, as a function of the wall variation.

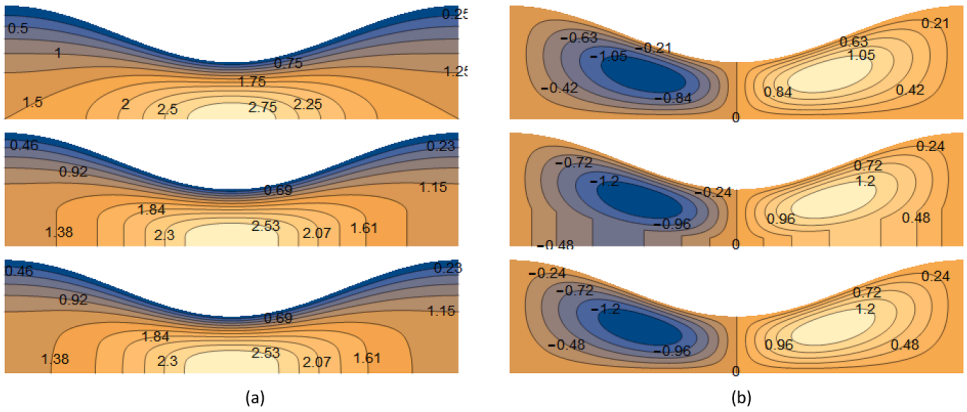

Fig. 7. (a) Axial and (b) transverse velocity contours in an undulating symmetric channel with λ=0.5 and $k = 1$ for a Newtonian fluid (Bn=0, top), Bingham fluid (Bn=2, middle), and Papanastasiou fluid (Bn=2 and $M = 10$, bottom).

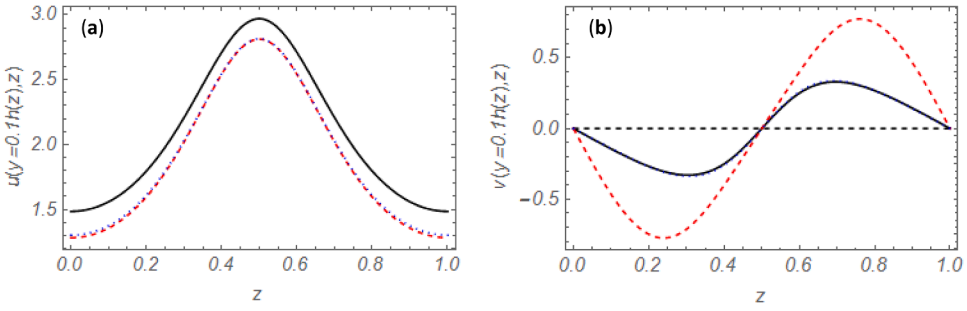

Fig. 8. (a) Axial and (b) transverse velocity at $y = 0.1h(z)$ in an undulating symmetric channel with λ=0.5 and $k = 1$ for a Newtonian fluid (Bn=0, black solid), Bingham fluid (Bn=2, red dotted), and Papanastasiou fluid (Bn=2 and $M = 10$, blue dashed). (For interpretation of the references to colour in this figure legend, the reader is referred to the web version of this article.)

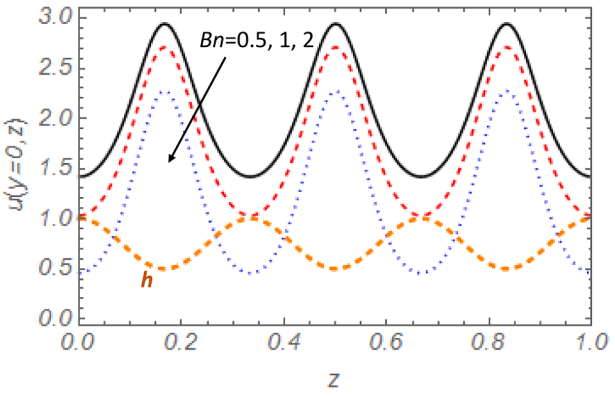

Fig. 9. The maximum (midplane) axial velocity (midplane velocity) in Papanastasiou flow with $M = 10$ and Bn=0.5 (black solid), 1 (red dashed), and 2 (blue dotted) in a symmetric undulating channel with λ=0.5 and $k = 3$. The wall function (Eq. (66)) is also plotted (lower orange dashed line). (For interpretation of the references to colour in this figure legend, the reader is referred to the web version of this article.)

it should be expected due to incompressibility and the total mass balance, and as the analytical solutions for the Newtonian and Bingham fluids show; of course, the same holds for the Papanastasiou fluid.

6. Conclusions

Based on the classic lubrication theory, we have derived an analytical solution of the 2D flow of a Papanastasiou fluid in symmetric ducts with variable cross-section. Our solution is valid at the lubrication limit (i.e. at a vanishing small aspect ratio of the duct) and under the assumption of a varying rigid wall that can be described with a continuous and differentiable function. It merely requires the solution/input from an algebraic equation which can trivially be solved numerically.

For suitable values of the Bingham number and the Papanastasiou exponential parameter, the solution reduces to the Newtonian or the ideal Bingham fluid solutions. The pressure-drop required to maintain the constant volumetric flowrate through the duct has also been obtained. Results for undulating and linearly varying symmetric channels and pipes have been presented and discussed. The increase of the required pressure-drop with the Bingham number is clearly seen in all cases.

Declaration of Competing Interest

The authors declare that they have no known competing financial interests or personal relationships that could have appeared to influence the work reported in this paper.

Data availability

Data will be made available on request.

Appendix A. Asymptotic formulas for Bingham channel flow

An asymptotic formula for Φ for small values of the Bingham number can be found from Eq. (28):

$$\Phi|_{Bn\to 0} = \frac{3}{h^2} + \frac{3}{2}Bn - \frac{h^4}{18}Bn^3 + O\left(Bn^4\right) \tag{A1}$$

A similar analysis for large values of the Bingham number shows that:

$$\Phi|_{Bn\to \infty} = Bn + \frac{\sqrt{2}}{h}\sqrt{Bn} + \frac{4}{3h^2} + O\left(Bn^{-1/2}\right) \tag{A2}$$

From Eqs. (A1) and (A2) and the definition for Φ, we can trivially find $p'|_{Bn\to 0} = -\Phi|_{Bn\to 0}/h$ and $p'|_{Bn\to \infty} = -\Phi|_{Bn\to \infty}/h$. Moreover, using information from Eq. (A1) up to $O(Bn^2)$ and from Eq. (A2) up to $O(Bn^{1/2})$, we can also construct a two-point Padé approximant, Φ_a, of uniform convergence over the entire range of Bingham number, $0 \le Bn < \infty$, as described in a recent paper by Housiadas [21]:

$$\Phi_a = \frac{3/h^2 + (15/7)Bn + (9/(7h))\sqrt{2Bn} + 9h/\left(7\sqrt{2}\right)Bn^{3/2} + \left(3h^2/14\right)Bn^2}{1 + (3h/7)\sqrt{2Bn} + \left(3h^2/14\right)Bn} \tag{A3}$$

By means of (A1) and (A2), one gets the asymptotic formulas for the required pressure drop as Bn goes to zero and infinity, respectively:

$$\Delta\bar{p}|_{Bn\to 0} = \underbrace{6\int_0^1 \frac{dz}{h^3(z)}}_{\Delta\bar{p}_N} + 3Bn\int_0^1 \frac{dz}{h(z)} - \frac{Bn^3}{9}\int_0^1 h^3(z)dz + O\left(Bn^4\right) \tag{A4}$$

and

$$\Delta\bar{p}|_{Bn\to \infty} = 2Bn\int_0^1 \frac{dz}{h(z)} + 2\sqrt{2Bn}\int_0^1 \frac{dz}{h^2(z)} + \underbrace{\frac{8}{3}\int_0^1 \frac{dz}{h^3(z)}}_{4\Delta\bar{p}_N}/9 + O\left(Bn^{-1/2}\right) \tag{A5}$$

The simple formulas (A4) and (A5) should be compared with the exact solution, Eq. (64), and the approximate formula for $\Delta\bar{p}_B$ based on Φ_a as given by Eq. (A3), namely $\Delta\bar{p}_{B,a} = 2\int_0^1 (\Phi_a(z)/h(z))dz$.

Substituting Eq. (66) into Eq. (68), one finds at small Bn number:

$$\Delta\bar{p}_B|_{Bn\to 0} = \Delta\bar{p}_N + \frac{3}{\sqrt{1-\lambda}}Bn - \frac{(2-\lambda)\left(8-8\lambda+5\lambda^2\right)}{144}Bn^3 + O\left(Bn^4\right) \tag{A6}$$

At large Bn, one finds:

$$\Delta\bar{p}_B|_{Bn\to \infty} = \frac{2Bn}{\sqrt{1-\lambda}} + \frac{2-\lambda}{(1-\lambda)^{3/2}}\sqrt{2Bn} + \frac{4}{9}\Delta\bar{p}_N + O\left(Bn^{-1/2}\right) \tag{A7}$$

Notice that the wavenumber k which appears in the shape function does not appear in the formulas for $\Delta\bar{p}_N$ [20], $\Delta\bar{p}_B|_{Bn\to 0}$ and $\Delta\bar{p}_B|_{Bn\to \infty}$.

Similarly, substituting Eq. (69) into Eq. (68), gives:

$$\Delta\bar{p}_B|_{Bn\to 0} = \Delta\bar{p}_N + \frac{\ln(1+\delta h)^3}{\delta h}Bn - \frac{(2+\delta h)\left(2+2\delta h+\delta h^2\right)}{36}Bn^3 + O\left(Bn^4\right) \tag{A8}$$

and

$$\Delta\bar{p}_B|_{Bn\to \infty} = 2\left(\frac{\ln(1+\delta h)}{\delta h}Bn + \frac{\sqrt{2Bn}}{1+\delta h} + \frac{2}{9}\Delta\bar{p}_N\right) + O\left(Bn^{-1/2}\right) \tag{A9}$$

where $\Delta\bar{p}_N = 3(1+\delta h)/(2+\delta h)^2$ (see Eq. (67)). Finally, notice that for a straight channel $\lambda = 0$ (or $\delta h = 0$) and Eqs. (A6)-(A7) (or (A8)-(A9)) reduce to:

$$\Delta\bar{p}_B|_{Bn\to 0}(\lambda=0) = 6 + 3Bn - Bn^3/9 + O\left(Bn^4\right) \tag{A10}$$

and

$$\Delta\bar{p}_B|_{Bn\to \infty}(\lambda=0) = 2Bn + 2\sqrt{2Bn} + 8/3 + O\left(Bn^{-1/2}\right) \tag{A11}$$

The approximate formula for Φ can also be used over the entire range of the Bingham number; set $h = 1$ in Eq. (A3).

Appendix B. Asymptotic formulas for Bingham pipe flow

Asymptotic formulas for Φ as $Bn\to 0^+$ and as $Bn\to\infty$ can be found from Eq. (36):

$$\Phi|_{Bn\to 0} = \frac{8}{h^3} + \frac{4}{3}Bn - \frac{h^9}{1536}Bn^4 + O\left(Bn^5\right) \tag{B1}$$

and

$$\Phi|_{Bn\to \infty} = Bn + \frac{2}{h^{3/2}}\sqrt{Bn} + \frac{10}{3h^3} + O\left(Bn^{-1/2}\right) \tag{B2}$$

From Eqs. (B1) and (B2) and the definition for Φ, gives $p'|_{Bn\to 0} = -(2/h)\Phi|_{Bn\to 0}$ and $p'|_{Bn\to\infty} = -(2/h)\Phi|_{Bn\to\infty}$, respectively. Also, a two-point Padé-approximant based on Eqs. (B1) and (B2), can be constructed as described in Ref. [21], however due to its complexity is not advantageous compared to the exact analytical solution.

For the ideal Bingham fluid, the asymptotic formulas for the pressure drop give:

$$\Delta\bar{p}_B|_{Bn\to 0} = \underbrace{8\int_0^1 \frac{dz}{h^4(z)}}_{\Delta\bar{p}_N} + \frac{4}{3}Bn\int_0^1 \frac{dz}{h(z)} - \frac{Bn^4}{1536}\int_0^1 h^8(z)dz + O\left(Bn^5\right) \tag{B3}$$

and

$$\Delta\bar{p}_B|_{Bn\to \infty} = Bn\int_0^1 \frac{dz}{h(z)} + 2\sqrt{Bn}\int_0^1 \frac{dz}{h^{5/2}(z)} + \underbrace{\frac{10}{3}\int_0^1 \frac{dz}{h^4(z)}}_{5\Delta\bar{p}_N}/12 + O\left(Bn^{-1/2}\right) \tag{B4}$$

For the undulating pipe (Eq. (66)), one obtains:

$$\Delta\bar{p}_B|_{Bn\to 0} = \Delta\bar{p}_N + \frac{4}{3\sqrt{1-\lambda}}Bn - \frac{\Delta\bar{p}_4}{1536}Bn^4 + O\left(Bn^5\right) \tag{B5}$$

and

$$\Delta\bar{p}_B|_{Bn\to \infty} = \frac{Bn}{\sqrt{1-\lambda}} + 2\sqrt{Bn}\int_0^1 \frac{dz}{h^{5/2}(z)} + \frac{5}{12}\Delta\bar{p}_N + O\left(Bn^{-1/2}\right) \tag{B6}$$

where $\Delta\bar{p}_N$ is given by Eq. (67) and

$$\Delta\bar{p}_4 = 1 - 4\lambda + \frac{21\lambda^2}{2} - \frac{35\lambda^3}{2} + \frac{1225\lambda^4}{64} - \frac{441\lambda^5}{32} + \frac{1617\lambda^6}{256} - \frac{429\lambda^7}{256} + \frac{6435\lambda^8}{32768}$$

Likewise, for a pipe of linearly varying radius, one finds:

$$\Delta\bar{p}_B|_{Bn\to 0} = \Delta\bar{p}_N + \frac{4\ln(1+\delta h)}{3\,\delta h}Bn + \frac{1-(1+\delta h)^9}{13824\,\delta h}Bn^4 + O\left(Bn^5\right) \tag{B7}$$

and

$$\Delta\bar{p}_B|_{Bn\to \infty} = \frac{\ln(1+\delta h)}{\delta h}Bn + \frac{(1+\delta h)^{3/2}-1}{3\delta h(1+\delta h)^{3/2}}4\sqrt{Bn} + \frac{5}{12}\Delta\bar{p}_N + O\left(Bn^{-1/2}\right) \tag{B8}$$

where $\Delta\bar{p}_N$ is given by Eq. (70). For $\delta h \to 0$ (or $\lambda = 0$), i.e., for $h = 1$, formulas (B3) and (B4) reduce to:

$$\Delta\bar{p}_B|_{Bn\to 0} = 8 + \frac{4}{3}Bn - \frac{Bn^4}{1536} + O\left(Bn^5\right) \tag{B9}$$

and

$$\Delta\bar{p}_B|_{Bn\to \infty} = Bn + 2\sqrt{Bn} + \frac{10}{3} + O\left(Bn^{-1/2}\right) \tag{B10}$$

respectively.

References

[1] P. Coussot, Slow flows of yield stress fluids: yielding liquids or flowing solids, Rheol. Acta 57 (2018) 1–14.
[2] I. Frigaard, Simple yield-stress fluids, Curr. Opinion Coll. Inter. Sci. 43 (2019) 80–93.
[3] D. Bonn, J. Paredes, M.M. Denn, L. Berthier, T. Divoux, S. Manneville, Yield stress materials in soft condensed matter, Rev. Mod. Phys. 89 (2017), 035005.
[4] N.J. Balmforth, I.A. Frigaard, G. Ovarlez, Yielding to stress: recent developments in viscoplastic fluid mechanics, Annu. Rev. Fluid Mech. 46 (2014) 121–146.
[5] E.C. Bingham, Fluidity and Plasticity, McGraw Hill, New-York, 1922.
[6] R.R. Huilgol, G.C. Georgiou, Fluid Mechanics of Viscoplasticity, 2nd Edition, Springer International Publishing (Verlag), Berlin, 2022.
[7] T.C. Papanastasiou, Flow of material with yied, J. Rheology 31 (1987) 385–404.
[8] I.A. Frigaard, D.P. Ryan, Flow of a viscoplastic fluid in a channel of slowly varying width, J. Non-Newtonian Fluid Mech. 123 (2004) 67–83.
[9] A. Putz, I.A. Frigaard, D.M. Martinez, On the lubrication paradox and the use of regularization methods for lubrication flows, J. Non-Newtonian Fluid Mech. 163 (2009) 62–77.
[10] L. Fusi, A. Farina, F. Rosso, S. Roscani, Pressure-driven lubrication flow of a Bingham fluid in a channel: a novel approach, J. Non-Newtonian Fluid Mech. 221 (2015) 66–75.
[11] L. Fusi, A. Farina, Peristaltic axisymmetric flow of a Bingham plastic, Appl. Math. Comp. 320 (2018) 1–15.
[12] L. Fusi, K.D. Housiadas, G.C. Georgiou, Flow of a Bingham fluid in a pipe of variable radius, J. Non-Newtonian Fluid Mech. 285 (2020), 104393.
[13] G.C. Georgiou, Singular Finite Elements For Newtonian flow Problems With Stress Singularities, The University of Michigan, 1989. Ph.D. thesis.
[14] R.M. Corless, G.H. Gonnet, D.G.E. Hare, D.J. Jeffray, D.E. Knuth, On the Lambert W function, Adv. Comput. Math. 5 (1996) 329–359.
[15] J. Lehtonen, The Lambert W function in ecological and evolutionary models, Methods Ecol. Evolut. 7 (1996) 1110–1118.
[16] Z. You, R.R. Huilgol, E. Mitsoulis, Application of the Lambert *W* function to steady shearing flows of the Papanastasiou model, Int. J. Engineering Sci. 46 (2008) 799–808.
[17] K.D. Housiadas, Improved convergence based on linear and non-linear transformations at low and high Weissenberg asymptotic analysis, J. Non-Newtonian Fluid Mech. 247 (2017) 1–14.
[18] R. Pitsillou, G.C. Georgiou, R.R. Huilgol, On the use of the Lambert function in solving non-Newtonian flow problems, Phys. Fluids 32 (2020), 093101.
[19] B. Tavakol, G. Froehlicher, D.P. Holmes, H.A. Stone, Extended lubrication theory: improved estimates of flow in channels with variable geometry, Proc. R. Soc. A 473 (2017), 20170234.
[20] K.D. Housiadas, C. Tsangaris, High order lubrication theory in channels and tubes with variable geometry, Acta Mech. 233 (10) (2022).
[21] K.D. Housiadas, Improved convergence based on two-point Padé approximants: simple shear, uniaxial elongation, and flow past a sphere, Phys. Fluids 247 (2023), 013101.